Statistical analysis of ^{18}F-fluorodeoxyglucose positron-emission tomography/computed tomography ground-glass nodule findings

KAZUYA NISHII[1,2], AKIHIRO BESSHO[1], NOBUAKI FUKAMATSU[1], YOSHIKO OGATA[1], SHINOBU HOSOKAWA[1], MAKOTO SAKUGAWA[1] and MITSUMASA KAJI[3]

[1]Department of Respiratory Medicine, Japanese Red Cross Okayama Hospital, Okayama, Okayama 700-8607; [2]Department of Hematology, Oncology and Respiratory Medicine, Okayama University Graduate School of Medicine, Dentistry and Pharmaceutical Sciences, Okayama, Okayama 700-8558; [3]Okayama Diagnostic Imaging Center, Okayama, Okayama 700-0913, Japan

Received April 3, 2018; Accepted June 29, 2018

DOI: 10.3892/mco.2018.1670

Abstract. ^{18}F-fluorodeoxyglucose positron-emission tomography/computed tomography (^{18}F-FDG-PET/CT) is important in lung cancer diagnosis; false negatives are often caused by ground-glass nodules (GGNs). PET/CT utility in GGN diagnosis is unknown. The associations between GGN CT findings (size, properties), the pathological diagnosis and maximum standardized uptake value (SUV_{max}) were explored. Sixty-six patients with pathological stage IA1-IIA lung adenocarcinoma underwent surgical resection and PET/CT between January 2010 and December 2014. Clinical characteristics, CT findings, pathological diagnoses and PET/CT findings were retrospectively examined. The age range was 47-86 years (median, 69 years), the female/male ratio was 38:28 and the pathological stage was IA1, IA2, IA3, IB and IIA in 5, 30, 21, 9 and 1, respectively. Total and solid-part lesion diameters ranged from 7.00-41.13 mm (median, 19.43 mm) and 0.00-23.23 mm (median, 4.55 mm), respectively; the solid-part ratio (solid-part diameter/total diameter) was 0-77% (median, 20%). SUV_{max} ranged from a value too low for evaluation to 3.9 (median, 1.0). Pathological diagnoses were adenocarcinoma *in situ* (AIS), minimally invasive adenocarcinoma (MIA), lepidic-predominant adenocarcinoma (LPA) and papillary predominant adenocarcinoma (PPA) in 17, 15, 32 and 2, respectively. Correlation coefficients for each factor and SUV_{max} for total and solid-part diameters were 0.513 ($p<0.0001$) and 0.461 ($p<0.0001$), respectively. All pure GGNs showed clinically unimportant $SUV_{max}<2.5$, even though some large GGNs were included (maximum, 40.0 mm). A total diameter ≥20 mm was significantly associated with FDG uptake ($p<0.0001$). SUV_{max} were <2.5 when the solid-part diameter was <4.55 mm. The AIS-MIA group showed significantly lower SUV_{max} than the LPA-PPA group ($p=0.0008$). There was no clinically important SUV_{max} with diagnostic value for pure or small part-solid GGNs. There were medium correlations for GGN total diameter, solid-part diameter, and SUV_{max}. We should note PET/CT's limitations in GGN diagnosis.

Introduction

^{18}F-fluorodeoxyglucose-positron emission tomography/computed tomography (^{18}F-FDG-PET/CT) is widely used to make qualitative diagnoses. When treating lung cancers, for example, it is used to determine the malignancy of lesions in the lungs and lymph nodes. However, PET images generally have poorer resolution than CT images and scans of lung tissue are particularly affected by respiratory rhythms. These factors are considered to limit PET's usefulness in diagnosing small-diameter lesions such as ground-glass nodules (GGNs (1-3). However, few publications have examined PET/CT's utility when examining GGNs alone (4,5). Moreover, it has not been established definitively whether this imaging modality is useful for certain kinds of GGNs and how such data should be evaluated. Well-differentiated adenocarcinomas are among the types of GGN lesions identifiable on CT. However, their small diameter makes it difficult to collect pathological specimens in many cases (for example, by means of bronchoscopy or CT-guided needle lung biopsy). This raises an important question regarding the utility of PET/CT for determining the benignity or malignancy of GGNs. In this study, we examined PET/CT's clinical utility for the diagnosis of GGN lesions by comparing preoperative CT and PET/CT findings of patients who underwent surgery at Japanese Red Cross Okayama Hospital and who were diagnosed with lung cancer based on histological findings.

Correspondence to: Dr Akihiro Bessho, Department of Respiratory Medicine, Japanese Red Cross Okayama Hospital, 2-1-1 Aoe Kita-ku Okayama, Okayama 700-8607, Japan
E-mail: abessho@okayama-med.jrc.or.jp

Abbreviations: AIS, adenocarcinoma *in situ*; ^{18}F-FDG-PET/CT, ^{18}F-fluorodeoxyglucose positron-emission tomography/computed tomography; GGN, ground-glass nodule; MIA, minimally invasive adenocarcinoma; LPA, lepidic-predominant adenocarcinoma; LSO, lutetium oxyorthosilicate; PPA, papillary-predominant adenocarcinoma; SUV_{max}, maximum standardized uptake value

Key words: lung cancer, adenocarcinoma, ground-glass nodule, PET/CT, SUV_{max}

Patients and methods

Records of patients diagnosed with lung cancer following pulmonary resection at Japanese Red Cross Okayama Hospital between January 2010 and December 2014 were reviewed retrospectively. Only patients who underwent PET/CT and whose preoperative CT findings indicated GGNs were analyzed.

All patients were imaged using an Aquilion 64 CT scanner at Japanese Red Cross Okayama Hospital (Toshiba Medical Systems, Otawara, Japan). The scan settings were as follows: slice dimensions = 512x512 pixels, slice thickness = 1.0 mm, scanning interval = 0.8 mm, tube voltage =120 mA (with automatic tube voltage modulation), and pitch factor = 0.844. GGNs were evaluated on horizontal chest CT images in terms of total diameter (the long axis of the lesion), solid-part diameter (the long axis of the hyperechoic, low-contrast part, as determined visually), and solid-part ratio (the solid-part diameter/total diameter) (Fig. 1). If multiple GGNs were observed simultaneously in a slice, only the lesion with the largest total diameter was analyzed.

PET/CT scanning was performed at Okayama Diagnostic Imaging Center and Okayama Kyokuto Hospital. At the former, patients were scanned using a lutetium oxyorthosilicate (LSO)-based Biograph Sensation 16 PET/CT scanner with manufacturer-recommended settings (Siemens, Munchen, Germany). FDG (3.7 MBq/kg) was administered intravenously after the patient had fasted for ≥5 h; scanning began 90 min thereafter. At the latter, patients were scanned using a Discovery LS PET/CT system with manufacturer-recommended settings (General Electric Company, Boston, MA, USA). FDG (6 MBq/kg) was administered intravenously after the patient had fasted for ≥4 h; scanning began 50 and 120 min thereafter for early- and delayed-phase images, respectively. Only early-phase images were used in the analysis. Both facilities conduct daily inspections for PET/CT quality control. Various studies have been published on the evaluation of PET findings. This study employed the maximum standardized uptake value (SUV_{max}), a commonly used metric in Japan at present. Pulmonary nodules were judged to have clinically important FDG uptake when the SUV_{max} was ≥2.5 (2,6).

The statistical analysis was performed using EZR software version 1.36 (Saitama Medical Center, Jichi Medical University, Saitama, Japan) (7). In the statistical analysis, an SUV_{max} too low to evaluate was treated as SUV_{max}=0.0. $p \leq 0.05$ was considered to indicate a statistically significant difference in two-group comparisons. Correlations were evaluated using the Pearson product-moment correlation coefficient; $r \geq 0.4$ was considered to indicate a moderate correlation. Fischer's exact test was used to analyze frequency distributions. The t-test was used to determine whether differences in the means of two sets of samples were significant.

All lung cancer diagnoses were corroborated by the pathological histology of the biopsied specimens. Original histology-based diagnoses were based on the General Rules for the Clinical and Pathological Classification of Lung Cancer of the Japan Lung Cancer Society (8th edition) and the TNM staging system of the International Association for the Study of Lung Cancer (8th edition) (8). The same tissue specimens were re-examined and classified in the present study using the World Health Organization Classification of Tumors of the Lung, Pleura, Thymus, and Heart (4th edition) (9).

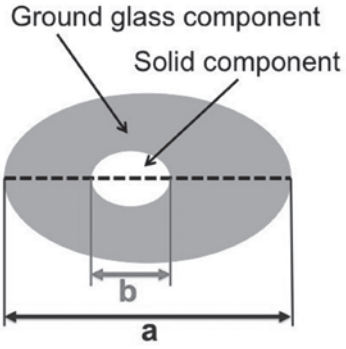

Figure 1. CT findings (Part-solid GGN). Symbols: a, Total diameter; b, Solid-part diameter; b/a, Solid-part ratio.

Table I. Patient characteristics (n=66).

Features	No.
Median age, year (range)	69 (47-86)
Sex (female/male)	38/28
Histology (AIS/MIA/LPA/PPA)	17/15/32/2
pT stage (1a/1b/1c/2a/2b)	30/5/21/9/1
Mean total diameter, mm (range)	19.43 (7.0-41.13)
Mean solid-part diameter, mm (range)	4.55 (0-23.23)
Mean SUV_{max}, (range)	1.0 (insignificant – 3.9)

AAH, atypical adenomatous hyperplasia, AIS, adenocarcinoma *in situ*; MIA, minimally invasive adenocarcinoma; LPA, lepidic predominant adenocarcinoma; PPA, papillary predominant adenocarcinoma.

Patients' clinical characteristics, CT findings (total diameter, solid-part diameter, and solid-part ratio), pathological diagnosis, and their relationships with the SUV_{max} were analyzed statistically. This study was conducted with the approval of the Ethics Committee of Japanese Red Cross Okayama Hospital.

Results

In total, 66 patients who were diagnosed with lung cancer following pulmonary resection at Japanese Red Cross Okayama Hospital between January 2010 and December 2014 were analyzed. All had undergone PET/CT and had preoperative CT findings indicating GGNs. The subjects ranged in age from 47-86 years (median, 69 years) and consisted of 28 men and 38 women. All were diagnosed with lung adenocarcinoma; lymph node/distant metastasis was not observed in any case. The pathologic tumor (pT) factors were 1a, 1b, 1c, 2a, and 2b in 5, 30, 21, 9, and 1 case(s), respectively; the pathologic stage (pStage) classifications were IA1, IA2, IA3, IB, and IIA in 5, 30, 21, 9, and 1 case(s), respectively. Visceral pleural infiltration beyond the elastic layer was observed in one case but did not reach the visceral pleural membrane (i.e., stage pl1). The total diameters of the GGNs according to CT findings ranged from 7.0-41.13 mm (median, 19.43 mm); the solid-part diameters ranged from 0.0-23.23 mm (median, 4.55 mm), and

the solid-part ratios ranged from 0-77% (median, 20%). A total of 22 lesions were diagnosed as pure GGNs. The SUV_{max} ranged from a value too low to be evaluated to a maximum of 3.9 (median, 1.0). The SUV_{max} ranged from 1.00-1.49 in 34 patients (51.5%), 1.50-1.99 in 19 (28.8%), 2.00-2.49 in 11, (16.7%), and ≥2.5 in 6 (9.1%). The histopathological classifications of the adenocarcinoma subtype were adenocarcinoma *in situ* (AIS) in 17 patients, minimally invasive adenocarcinoma (MIA) in 15, lepidic-predominant adenocarcinoma (LPA) in 32, and papillary-predominant adenocarcinoma (PPA) in 2 (10) (Table I). The SUV_{max} correlated with each CT metric as follows: r=0.513 for the total diameter (p<0.0001), r=0.461 for the solid-part diameter, and r=0.307 for the solid-part ratio (p<0.0001). Patients with total GGN diameters ≥20 mm were significantly more likely to have an SUV_{max}≥2.5 than were patients with smaller lesions (p<0.0001). No pure GGN or lesion with a solid-part diameter <4.55 mm exhibited an SUV_{max}≥2.5. Eight tumors with an SUV_{max}<2.5 were classified as pure GGNs (AIS, 3; MIA, 4; and LPA, 2). There was no significant difference in the frequency of SUV_{max}≥2.5 in the AIS-MIA group and the LPA-PPA group (p=0.198) (Table II). All had an SUV_{max}≥1.0 and comprised 38.1% of all pure GGNs observed. The AIS-MIA group showed a significantly lower SUV_{max} than the LPA-PPA group (p=0.0008). The average value of SUV_{max} in each group was 0.61 (95% confidence interval 0.309-0.919) in the AIS-MIA group and 1.43 (95% confidence interval 1.07-1.789) in the LPA-PPA group (Fig. 2).

Table II. SUV-max distributions by adenocarcinoma classification (n=66).

SUV_{max}	<1.0	1.0-1.4	1.5-1.9	2.0-2.4	≥2.5	≥2.5 (%)[a]
AIS	10	4	1	1	1	5.8
MIA	10	3	1	1		0
LPA	11	8	5	3	5	15.6
PPA	1		1			0

[a]There was no significant difference in the frequency of SUV_{max} ≥2.5 in the AIS-MIA group and the LPA-PPA group (p=0.198). AAH, atypical adenomatous hyperplasia; AIS, adenocarcinoma *in situ*; MIA, minimally invasive adenocarcinoma; LPA, lepidic predominant adenocarcinoma; PPA, papillary predominant adenocarcinoma.

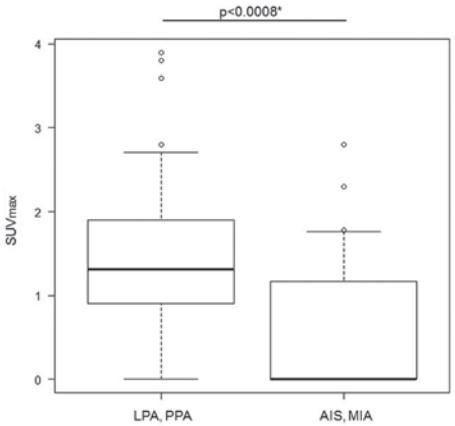

Figure 2. Comparison of SUV_{max} by each tissue type. *T-test. AIS, adenocarcinoma *in situ*; MIA, minimally invasive adenocarcinoma; LPA, lepidic predominant adenocarcinoma; PPA, papillary predominant adenocarcinoma.

Discussion

Our investigation observed a moderate correlation between the major-axis diameter and SUV_{max} of GGNs. The potential of using the SUV_{max} as a reference value was demonstrated by the fact that it was better correlated with the solid-part diameter than the total diameter. However, it is important to note that the correlation was low for pure GGNs and small-diameter lesions. Moreover, in some cases, imaging findings diverged from pathological findings; for example, one case was classified as AIS by postoperative histopathology despite the lesion having a solid part that had been observed before surgery. We did not use high-resolution CT (HR-CT) scanners, but the resolution of our CT images was typical for clinical scanning procedures. Nonetheless, perhaps this divergence would have been less had our scans been performed with greater precision using such equipment.

In this study, we also examined the relationship between AIS, MIA, LPA, PPA and SUV_{max}. There was a significant difference in the mean value of SUV_{max} in the AIS-MIA group and the LPA-PPA group, but the clear cut-off value is still unknown. Although the possibility of SUV_{max} 1.0 being a point dividing the two groups was shown in this study, and care should be taken for GGNs with SUV_{max} higher than that, further investigation is necessary in the future.

Normal lung tissue has an SUV_{max} of 0.6 (range, 0.2-1.8) and many past studies have used the criterion of an SUV_{max}>2.5 to diagnose a finding as malignant when performing PET/CT examinations of pulmonary nodules (11). Since we did not analyze noncancerous lesions in this study, the sensitivity in detecting cancer of SUV_{max}≥2.5 is unknown. However, in this study, even in the LAP-PPA group, the mean value of SUV_{max} is <2.5; thus, at least for GGN lesions, it is not an indicator for a non-carcinoma. The SUV is a semi-quantitative value that is affected by factors such as body type, blood sugar levels, and scanning time, and can further vary between different devices or image reconstruction software packages. Because of its simplicity and intuitiveness, it is widely used in clinical procedures to complement visual assessments such as the maximum intensity projection. Even though we analyzed PET/CT scans that were performed at two hospitals, we decided that since the SUV_{max} was measured at both locations, it could be used as a major assessment measure with a certain level of objectivity. However, we cannot deny the possibility that using scanning data from multiple institutions could have influenced our assessment. The SUV tends to be low in cells with low glucose metabolism on PET images, for example, highly differentiated lung adenocarcinomas and hepatocellular, renal, prostate, and gastric cancers. Past investigations have found that pure GGNs exhibit median SUV values of around 1.0 (4,12); our SUV_{max} data were not greatly divergent from these values. In addition, PET has low spatial resolution (7-8 mm), making it difficult to assess nodules less than 10 mm in diameter, generally speaking (2,13,14). Moreover, one study found that the SUV_{max} of lung carcinomas showing localized ground-glass opacities

was not significantly different from the SUV_{max} observed from inflammatory lesions (5). Therefore, we advise caution when using the SUV_{max} to determine the benignity or malignancy of lung cancers.

PET/CT-based research is becoming more diverse and is utilized in conjunction with a variety of different objectives and use cases. For example, one recent study found that the preoperative SUV could serve as a prognostic factor in c-stage IA lung adenocarcinomas (15). Technological advances are helping to increase the diagnostic accuracy of PET/CT; recent efforts have focused on developing image reconstruction techniques, improving spatial resolution by means of time-of-flight methods, and reducing partial-volume effects (16,17). While the clinical value of PET/CT in evaluating GGNs is still limited at present, it could increase in the future, and thus its evolution must be monitored carefully going forward.

This study is novel in that SUV_{max} was analyzed based on currently used pathological classifications of lung adenocarcinoma, suggesting the possibility of SUV_{max} value in lesions with higher malignancy, even in GGN lesions. In order to scientifically confirm the relationship between pathological findings and SUV_{max} values, future larger-scale prospective observational research with a focus on similar imaging conditions is necessary.

This study was presented at the 2015 World Conference on Lung Cancer (Denver, CO, USA).

Acknowledgements

Not applicable.

Funding

No funding was received.

Availability of data and materials

The datasets generated during and/or analyzed during the current study are not publicly available to protect the patients' personal information but are available from the corresponding author for reasonable requests.

Authors' contributions

KN, AB, NF, YO, SH, MS and MK conceived of and designed the research. KN and AB analyzed and interpreted the data. KN and AB wrote and revised the manuscript. All authors read and approved the final manuscript.

Ethics approval and consent to participate

This study was conducted with the approval of the Ethics Committee of Japanese Red Cross Okayama Hospital. The requirement for informed consent was waived by the ethics committee because of the study's retrospective nature; however, patients could opt out of sharing their information.

Patient consent for publication

Not applicable.

Competing interests

The authors declare that they have no competing interests.

References

1. Naidich DP, Bankier AA, MacMahon H, Schaefer-Prokop CM, Pistolesi M, Goo JM, Macchiarini P, Crapo JD, Herold CJ, Austin JH, *et al*: Recommendations for the management of subsolid pulmonary nodules detected at CT: a statement from the Fleischner Society. Radiology 266: 304-317, 2013.
2. Gould MK, Maclean CC, Kuschner WG, Rydzak CE and Owens DK: Accuracy of positron emission tomography for diagnosis of pulmonary nodules and mass lesions: a meta-analysis. JAMA 285: 914-924, 2001.
3. Nomori H, Watanabe K, Ohtsuka T, Naruke T, Suemasu K and Uno K: Evaluation of F-18 fluorodeoxyglucose (FDG) PET scanning for pulmonary nodules less than 3 cm in diameter, with special reference to the CT images. Lung Cancer 45: 19-27, 2004.
4. Kim TJ, Park CM, Goo JM and Lee KW: Is there a role for FDG PET in the management of lung cancer manifesting predominantly as ground-glass opacity? AJR Am J Roentgenol 198: 83-88, 2012.
5. Chun EJ, Lee HJ, Kang WJ, Kim KG, Goo JM, Park CM and Lee CH: Differentiation between malignancy and inflammation in pulmonary ground-glass nodules: the feasibility of integrated ^{18}F-FDG PET/CT. Lung Cancer 65: 180-186, 2009.
6. Vansteenkiste J and Dooms C: Positron emission tomography in nonsmall cell lung cancer. Curr Opin Oncol 19: 78-83, 2007.
7. Kanda Y: Investigation of the freely available easy-to-use software 'EZR' for medical statistics. Bone Marrow Transplant 48: 452-458, 2013.
8. Goldstraw P, Chansky K, Crowley J, Rami-Porta R, Asamura H, Eberhardt WE, Nicholson AG, Groome P, Mitchell A, Bolejack V, *et al*: The IASLC Lung Cancer Staging Project: proposals for revision of the TNM stage groupings in the forthcoming (Eighth) edition of the TNM Classification for Lung Cancer. J Thorac Oncol 11: 39-51, 2016.
9. Travis WD, Brambilla E, Nicholson AG, Yatabe Y, Austin JHM, Beasley MB, Chirieac LR, Dacic S, Duhig E, Flieder DB, *et al*: The 2015 World Health Organization Classification of Lung Tumors: Impact of Genetic, Clinical and Radiologic Advances Since the 2004 Classification. J Thorac Oncol 10: 1243-1260, 2015.
10. Travis WD, Brambilla E, Noguchi M, Nicholson AG, Geisinger KR, Yatabe Y, Beer DG, Powell CA, Riely GJ, Van Schil PE, *et al*: International Association for the Study of Lung Cancer/American Thoracic Society/European Respiratory Society international multidisciplinary classification of lung adenocarcinoma. J Thorac Oncol 6: 244-285, 2011.
11. Patz EF Jr, Lowe VJ, Hoffman JM, Paine SS, Burrowes P, Coleman RE and Goodman PC: Focal pulmonary abnormalities: evaluation with F-18 fluorodeoxyglucose PET scanning. Radiology 188: 487-490, 1993.
12. Wu HB, Wang L, Wang QS, Han YJ, Li HS, Zhou WL and Tian Y: Adenocarcinoma with BAC features presented as the nonsolid nodule is prone to be false-negative on 18F-FDG PET/CT. Biomed Res Int 2015: 243681, 2015.
13. Lindell RM, Hartman TE, Swensen SJ, Jett JR, Midthun DE, Nathan MA and Lowe VJ: Lung cancer screening experience: a retrospective review of PET in 22 non-small cell lung carcinomas detected on screening chest CT in a high-risk population. AJR Am J Roentgenol 185: 126-131, 2005.
14. Cronin P, Dwamena BA, Kelly AM and Carlos RC: Solitary pulmonary nodules: meta-analytic comparison of cross-sectional imaging modalities for diagnosis of malignancy. Radiology 246: 772-782, 2008.
15. Hattori A, Suzuki K, Matsunaga T, Fukui M, Tsushima Y, Takamochi K and Oh S: Tumour standardized uptake value on positron emission tomography is a novel predictor of adenocarcinoma in situ for c-Stage IA lung cancer patients with a part-solid nodule on thin-section computed tomography scan. Interact Cardiovasc Thorac Surg 18: 329-334, 2014.
16. Suljic A, Tomse P, Jensterle L and Skrk D: The impact of reconstruction algorithms and time of flight information on PET/CT image quality. Radiol Oncol 49: 227-233, 2015.
17. Akamatsu G, Ishikawa K, Mitsumoto K, Taniguchi T, Ohya N, Baba S, Abe K and Sasaki M: Improvement in PET/CT image quality with a combination of point-spread function and time-of-flight in relation to reconstruction parameters. J Nucl Med 53: 1716-1722, 2012.